Clay Minerals, (2017) **52**, 453–468

The mineralogy and firing behaviour of pottery clays of the Lake Van region, eastern Turkey

A. ARAS[1,*] AND S. KILIÇ[2]

[1] *Department of Geological Engineering, Yüzüncü Yıl University, Van 65080, Turkey*
[2] *Department of Archaeology, Yüzüncü Yıl University, Van 65080, Turkey*

(*Received 20 May 2017; revised 11 December 2017; Associate Editor: Asuman Turkmenoglu*)

ABSTRACT: The present study focused on the mineralogical and chemical characterization and firing behaviour of clays from the Lake Van region and compared them with the same characteristics established for two ancient pot sherds. Four pottery clays collected from Kutki and Kuşluk in the Kesan Valley to the south, from Kavakbaşı to the southwest and from Bardakçı village on the east coast of Lake Van were analysed by X-ray diffraction to identify mineralogical composition (bulk clays and <2 μm fractions after heating at 300–500°C and ethylene glycol solvation). Further analyses were conducted to determine the size distribution, chemical composition and physical properties of test bodies derived from these clays. The *in situ* weathered schist forming the primary micaceous red clays which are suitable for local pottery production are characterized by large muscovite-sericite-illite and small calcite contents. In contrast, the Bardakçı clays are dominated by large smectite contents and are only used sparingly in mixtures of local pottery production because they undergo firing shrinkage and present drying and firing flaws in the fired bodies. Firing ranges of ~800–900°C were inferred from the mineralogy and colours of the two ancient sherds from Kutki. As a result of mineralogical analysis of fired and unfired test bodies of these pottery clays and pot sherds, two different types of pastes were determined for pottery production in the Lake Van region: metamorphic and volcanic paste, the former characterized by a calcite-poor and mica-sericite-rich matrix and the latter by large smectite and small calcite contents.

KEYWORDS: Lake Van, pottery, mineralogy, smectite, muscovite-sericite-illite, traditional kiln.

The Lake Van region is situated on the high plateaus of eastern Turkey, north of Upper Mesopotamia which has several sites, ruins and monuments which belonged to ancient civilizations. The oldest ceramic examples were defined locally and named "Tilkitepe Ware" and have red painted decoration with wavy or straight parallel lines on the outer surface from the mouth downwards (Korfmann, 1982). There are also examples of black burnished, handmade and mineral-tempered pottery which belong to the early Bronze Age culture of "Kura-Araxes" or "Karaz" (Burney, 1958; Korfmann, 1982). The Urartu Kingdom (800–600 BC) was located in the highlands between Anatolia, Mesopotamia and the Caucasian mountains. Regional prehistoric and traditional ceramic examples (Kılıç & Çalışkan, 2005) and a group of Urartian and Roman ceramic pieces collected from the castle of Van (Akça *et al*. 2010) have been analysed in a number of archaeometry projects. Sakarya *et al*. (1990) examined 12th and 13th century ceramics from Samsat, in southeastern Turkey, and the same research group

This paper is one of a group published in this issue which was originally presented at the Mediterranean Clay Conference, held in Izmir, Turkey in September 2016.
* E-mail: aras5549@yahoo.com
https://doi.org/10.1180/claymin.2017.052.4.04

(Kapur *et al.*, 1992) also examined an assemblage of Chalcolithic–early Bronze Age ceramics from Ikiztepe in Turkey. Both studies used XRD to define the mineral phases and to constrain the firing temperatures, but neither defined the provenance. The important archaeological questions about ancient pottery production in these historical sites are how, where and when they were produced. The answers to these questions should begin with knowledge of the local geology and local clay raw materials and other natural sources used in pottery production. The mineralogy of all clay sources in western Turkey has been studied extensively and documented in the literature because of the well developed ceramics industry, but there have been no studies of clay sources or of the provenance of historical ceramics from eastern or southeastern Turkey. The contemporary pottery production centres from the Lake Van area are situated mostly to the south and southwest of the Lake, except for Bardakçı village which is on the east coast. These centres have developed around suitable red clay deposits to the south and southwest of Lake Van in Kutki, Kuşluk and Kavakbaşı villages in the south and in Bardakçı to the east. It is possible to examine the production process of ancient pots in works taken from these local ceramic production centres around Lake Van. The present study attempted to determine the local clay sources and the mineralogical composition and firing behaviours of these clays and other production-related processes such as firing temperature and atmosphere, *i.e.* kiln type. An additional goal was the characterization of the mineralogical composition and physical properties of test bodies derived from these local clays and the preparation of data sources for researchers of ancient sherds.

GEOLOGICAL SETTING OF CLAY RAW MATERIALS

The centres of pottery production developed around suitable sources of clay raw materials in the Lake Van region. Therefore, the clay sources are labelled with the name of the nearest village and are shown in Fig. 1. The rocks around Lake Van consist of the E–W-trending metamorphic Bitlis complex rocks of Palaeozoic age along the S–SW coast of the lake, the linear Quaternary volcanic chain (Fig. 1) extending along the N–NW shore of Lake Van with Nemrut and Suphan volcanoes and the rather gentle hillside topography composed of Cretaceous ophiolitic mélanges and Tertiary sediments in the east coast (Fig. 1) (Degens & Kurtman, 1978). A generalized lithostratigraphic section of the Bitlis complex consists of the following (from bottom to top): the pre- to infra-Cambrian Hizan group, composed of gneisses, metabasic rocks and schists, which is separated into three formations: the Andok augengneiss with biotite, muscovite, amphibole; the Unaldi formation with amphibolites and garnet-amphibolites with relics of eclogite (Okay *et al.* 1985); and the Ohin schists

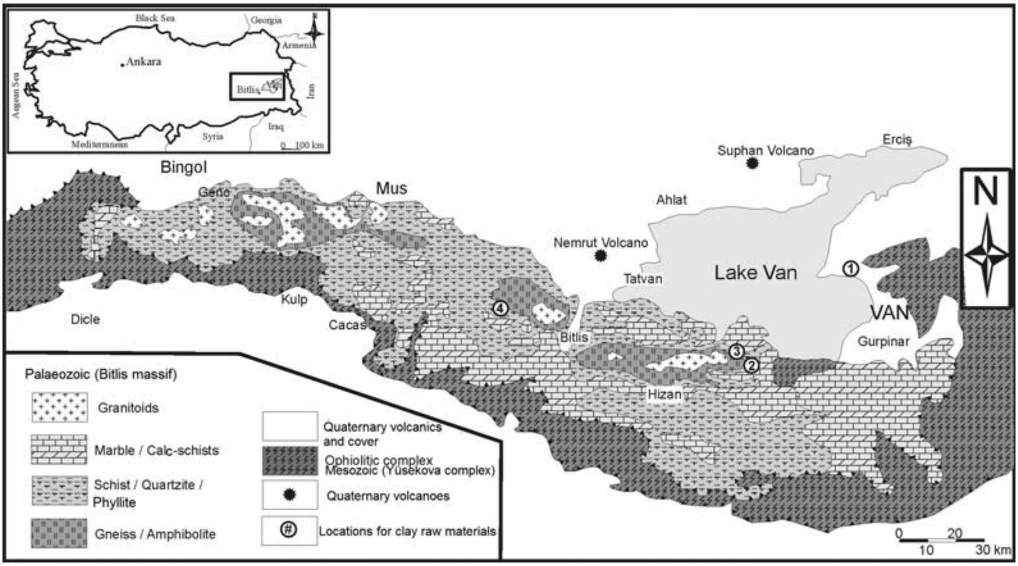

FIG. 1. Pottery clay locations in the Lake Van region from: (1) Bardakçı; (2) Kutki; (3) Kuşluk; and (4) Kavakbaşı shown in the geological map of the Bitlis Massif (modified from Altınlı, 1966 and Oyan & Tolluoğlu, 2005).

https://doi.org/10.1180/claymin.2017.052.4.04 Published online by Cambridge University Press

containing biotite, muscovite, garnet and amphibole (*e.g.* Göncüoğlu &Turhan, 1984; Oberhänsli *et al*., 2009). The first pottery production centre in Bardakçı village is situated on the east coast of Lake Van. The Bardakçı samples were collected from the Quaternary Lake Van terrace (Kuzucuoğlu *et al*., 2010) which consists mainly of finely laminated clay and silt deposits with the clay-rich levels tempered by local potters with silty and sandy materials (Fig. 1). The Kavakbaşi and Kutki locations are situated in the metamorphic Ohin schist and the Kuşluk clay location is situated on a young Quaternary terrestrial fan deposit derived mainly from the Ohin schist (Fig. 1).

MATERIALS AND METHODS

Materials and analytical methods

The clays sampled were initially dried at 110°C and then crushed manually to reduce the grain size of large agglomerates. Mineralogical analysis was performed by X-ray diffraction (XRD) using a Philips PW 3710 diffractometer with Cu-$K\alpha$ radiation on powdered bulk samples and the <2 µm clay fraction. The relative abundance of non-clay minerals was estimated by comparing the intensity of the main peaks of the same minerals for the four powdered clay samples. For the clay-fraction analysis, the <2 µm fractions were separated by settling and mounted as oriented air-dried aggregates on glass slides. For each sample, five XRD patterns were recorded: bulk powder (Pow), air-dried (AD), ethylene-glycol (EG) solvated and heated at 300 and 550°C for 4 h (H).

Characteristic scanning electron microscopy (SEM) microstructures and energy-dispersive X-ray spectroscopy (EDS) elemental results of fractured surfaces of fired bodies were collected using an FEI Inspect F-50 SEM instrument which was equipped with an Energy Dispersive Spectrometer (EDAX). The microanalysis and SEM images were obtained from the surfaces of bodies fired at 900 and 1000°C which were fractured and gold-coated.

The grain-size distributions of four samples were measured from bulk samples using a Malvern Mastersizer-2000 laser diffraction particle analyzer. The samples were dispersed in 100 mL of deionized water, with no addition of dispersants, and disaggregated using a stirrer at 2000 rpm and by ultrasonic waves. The sand fraction (>20 µm), silt fraction (2–20 µm) and clay fraction (<2 µm) were calculated from the size-distribution curves.

Major-element chemical analysis was determined by X-ray fluorescence (XRF) spectrometry (Philips 1480 XRF) on pressed powder samples using USGS and CANMET certified standard materials.

Preparation of fired test bodies and firing in an electrical kiln

In order to determine the technological properties of the clays, 100 mm × 25 mm × 10 mm bodies with 8% moisture were moulded in a steel matrix and subjected to a pressure of 20 MPa using an hydraulic press. The unfired bodies were dried at 110°C and fired at 800, 900, 1000 and 1100°C in an electrical kiln with a heating rate of 5°C/min and a 2 h soaking time. Then the samples were cooled after turning off the kiln and the physical properties of four individual clay raw materials were measured from rectangular green and fired test bodies.

The colour parameters of the fired test bodies were measured using a Minolta spectrophotometer according to the La^*b^* system developed by Judd Hunter (standardized in 1976: DIN 6174, CIE-Lab, 1976), whereby L represents brightness, a^* represents redness-greenness and b^*, yellowness-blueness.

The linear firing shrinkage was evaluated using the formula: $[(lf - ld)/ld] \times 100$, where ld and lf are the measured length of the dried and fired samples (100 mm × 25 mm × 10 mm), respectively (TS 4790). The bending strength was measured using a three-point flexural strength test according to the Turkish Standard, TS 4790 (1986). The average values of the bending strength were calculated from the equation: $MF = 3FL/2bh2$, where: F is the breaking load (kg), L is the distance between supports (=29.67 mm), b is sample width (mm) and h is sample thickness (mm). The water absorption values were determined from heated and boiled ceramic samples according to Turkish standards TS-EN 771-1 (2015) and TS-EN 772-7 (1998), respectively. The pieces were soaked in water and heated until boiling point was reached. The ceramic bodies were separated from each other after being plunged into water in order to display the largest free surface possible and were kept in boiling water for 2 h. When the water reached 35–40°C, the ceramic bodies were taken out, their surfaces dried, and the bodies weighed. The value of the water absorption (WA) was calculated as follows: $WA = [(wf - wi)/wi] \times 100$ where wf = final weight; wi = initial weight.

RESULTS

Mineralogy of clay samples

In the Bardakçı area (Fig. 1), the mineralogical composition of the terrace deposit varied in the thinly

https://doi.org/10.1180/claymin.2017.052.4.04 Published online by Cambridge University Press

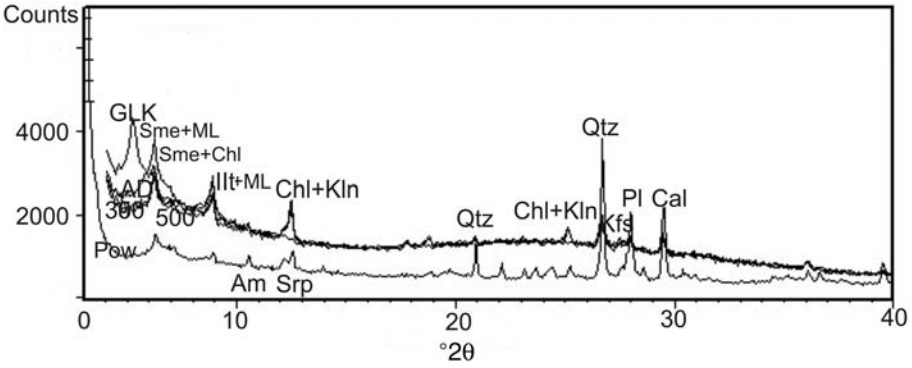

FIG. 2. XRD pattern of bulk powder (Pow) and air-dried (AD), ethylene glycol-solvated (GLK), heated (350, 550°C) oriented <2 µm fraction of Bardakçı clay (ML: mixed-layer, Qtz: quartz, Kln: kaolinite, Ill: illite, Chl: chlorite, Sme: smectite, Cal: calcite, Pl: plagioclase, Am: amphibole, Srp: serpentine, Kfs: K-feldspar).

bedded and fine-grained sandstone and within mudstone. The XRD pattern of the Bardakçı clay (mudstone) indicated the presence of quartz, calcite, serpentine, amphibole, muscovite-illite alkali feldspar and plagioclase as non-clay mineral phases.

Analysis by XRD of the clay fractions showed the presence of a broad 14–12 Å peak in the AD patterns which shifted to 16.8 Å in the EG-solvated samples, with weak 14 Å and 10 Å peaks remaining. The intensities of the latter peaks increased upon heating. Also, the 4.77 Å, and broad 7.20–7.10 Å and 3.58–3.52 Å peaks disappeared upon heating at 550°C. This observation indicates the presence of weathered chlorite together with kaolinite (Grim & Johns, 1954) and the coexistence of illite, mixed-layer illite-smectite and discrete smectite (Thorez, 1976) (Fig. 2D–E). Therefore, the clay-mineral assemblage of the Bardakçı clay includes discrete smectite, mixed-layer illite-smectite, illite, kaolinite and chlorite.

The Kavakbaşı samples contain quartz, K-feldspar, plagioclase and muscovite as non-clay minerals (Fig. 3). In the clay fraction the 14 Å peak shifted to 17–16 Å and formed a broad peak upon EG solvation indicating the presence of smectite. The small 14 Å peak in the EG-solvated, oriented clay fraction indicates the presence of chlorite. After heating, the 10 Å peak intensity increased and a very weak, broad peak remained at 12–11.8 Å indicating the presence of mixed-layer phases, probably mica-chlorite.

Quartz, K-feldspar and muscovite were detected as non-clay minerals in the powder XRD pattern of bulk Kusluk sediments (Fig. 4). In the XRD pattern of the

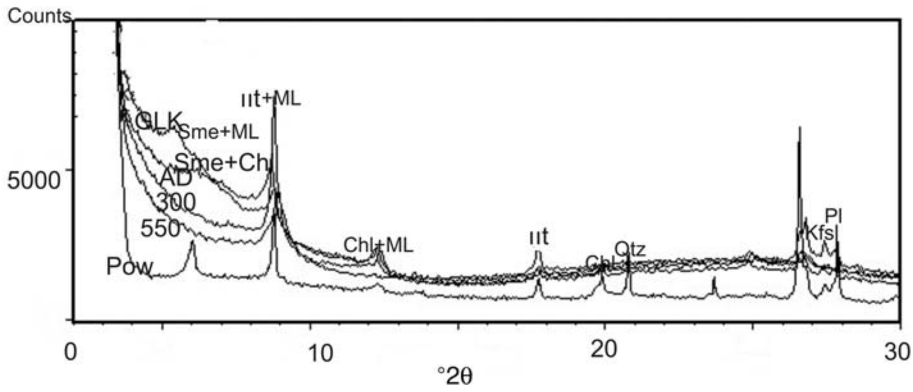

FIG. 3. XRD pattern of bulk powder (Pow), air-dried (AD), ethylene glycol-solvated (GLK), and heated (350, 550°C) oriented <2 µm fraction of Kavakbaşı clay (ML: mixed-layer, Qtz: quartz, Ill: illite, Chl: chlorite, Sme: smectite, Pl: plagioclase, Kfs: K-feldspar).

https://doi.org/10.1180/claymin.2017.052.4.04 Published online by Cambridge University Press

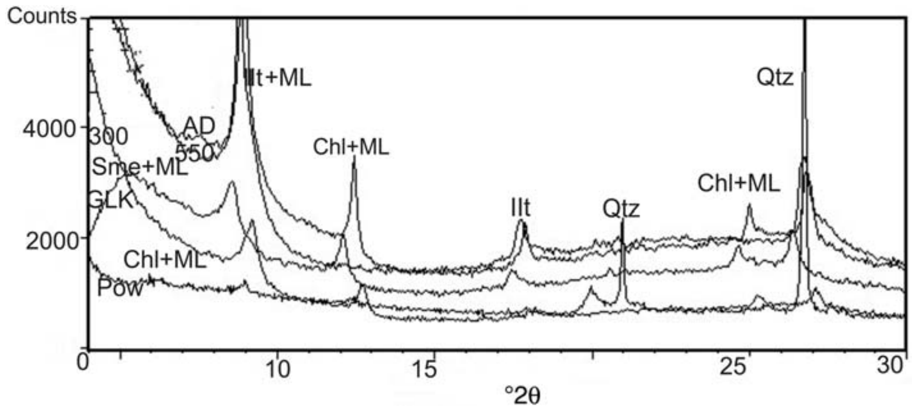

FIG. 4. XRD patterns of bulk powder sample (Pow), air-dried (AD), ethylene glycol-solvated (GLK), and heated (350, 550°C) mounts of oriented <2 μm fractions of Kusluk clay (ML: mixed-layer, Qtz: quartz, Ill: illite, Chl: chlorite, Sme: smectite, Pl: plagioclase, Kfs: K-feldspar).

oriented clay fraction, after EG treatment, the peak at 14 Å became broader and shifted to 17 Å, whereas after heating at 550°C, it collapsed to 10 Å. The 10 Å peak intensity increased and a new peak appeared at 12 Å whereas the 7.10 and 3.52 Å peaks disappeared. All these observations indicated the presence of a mixed-layer phase (probably mica-chlorite), discrete smectite and chlorite minerals (Grim & Johns, 1954; Thorez, 1976).

The K-feldspar, plagioclase and muscovite were detected as non-clay minerals in the powder XRD pattern of bulk Kutki clay (Fig. 5). After EG treatment, the 14 Å peak shifted to 17–18.4 Å, suggesting the presence of discrete smectite or/and random mixed-layer (ML) illite-smectite. The illite-mica peak at ~10 Å predominates in all patterns. The presence of a 13.8 Å peak upon heating at 350°C and the collapse of the 7.10 and 3.53 Å peaks upon heating at 550°C confirmed the presence of weathered chlorite (Grim & Johns, 1954).

XRD ANALYSIS RESULTS OF FIRED TEST BODIES DERIVED FROM THE POTTERY CLAYS

The XRD patterns of the powdered ceramic bodies derived from Bardakçı clay fired at 800, 900 and 1100°C are shown in Fig. 6. The calcite peak at 3.02 Å and the muscovite peaks at 10 and 5 Å remained at 800°C. At 900°C, the hematite peak appeared when calcite peaks disappeared and mica peaks were

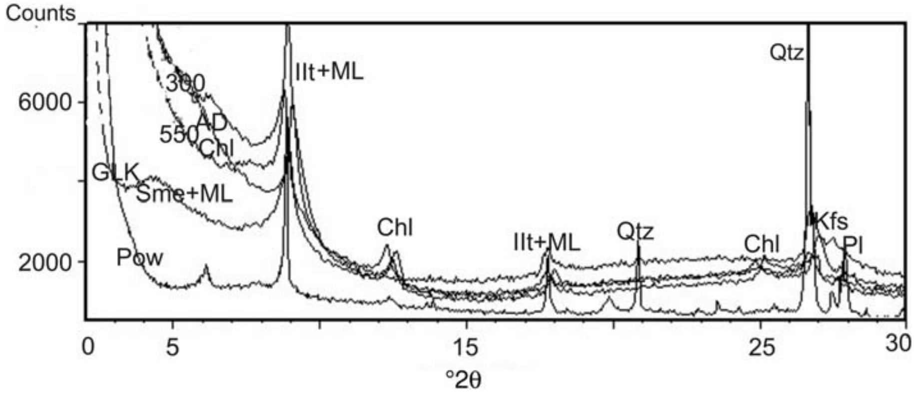

FIG. 5. XRD pattern of bulk powder (Pow), air-dried (AD), ethylene glycol-solvated (GLK), heated (350, 550°C) of oriented <2 μm fractions of Kutki clay (ML: mixed-layer illite-smectite, Qtz: quartz, Ill: illite, Chl: chlorite, Sme: smectite, Pl: plagioclase, Kfs: K- feldspar).

https://doi.org/10.1180/claymin.2017.052.4.04 Published online by Cambridge University Press

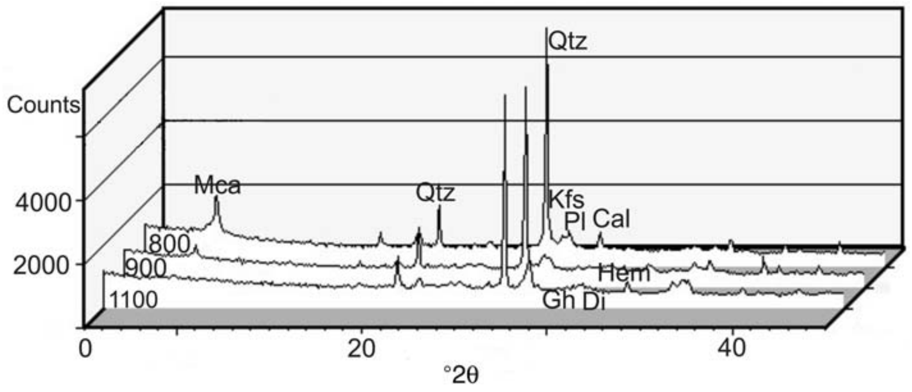

FIG. 6. XRD patterns of ceramic bodies derived from Bardakçı clay fired at various temperatures (Mca: mica, Qtz: quartz, Kfs: K-feldspar, Hem: hematite, Pl: plagioclase, Gh: gehlenite, Di: diopside, Cal: calcite).

preserved. At 1100°C, gehlenite (2.85 Å), diopside (2.90 Å) and plagioclase (3.19 Å) appeared and their abundances increased.

The XRD patterns of ceramic bodies derived from Kavakbaşı clay fired at various temperatures are given in Fig. 7. At 800°C, mica peaks were preserved and with increasing temperature, both types of feldspars melted and their intensities decreased. Hematite (2.67–2.51 Å) and gehlenite and diopside peaks appeared at 900°C.

The XRD patterns of ceramic bodies derived from Kusluk clay are given in Fig. 8. The observed mineral composition and evolution of mineral assemblages are similar in all weathered Kavabaşı, Kusluk and Kutki bodies; the only difference is the absence of gehlenite and diopside from the fired Kusluk body.

The XRD patterns of ceramic bodies derived from Kutki clay are shown in Fig. 9. The fired Kuşluk bodies display similar mineral assemblages to those in the Kutki bodies. The presence of very low relative intensities of quartz and the complete melting of feldspars and mica minerals dominate in the Kutki bodies.

SEM ANALYSIS OF CERAMIC BODIES DERIVED FROM THE POTTERY CLAYS

In the SEM images of fresh surfaces of the Bardakçı body fired at 1000°C (Fig. 10a,b), mica crystals have been preserved. The circular shape of the pores indicates the beginning of the development of a

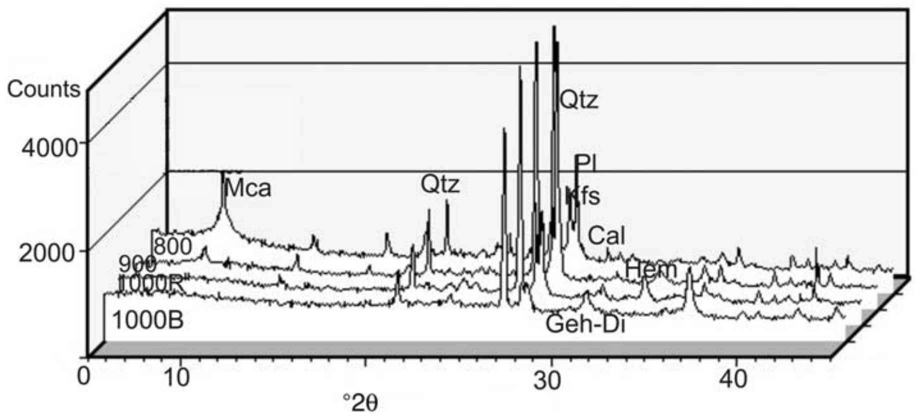

FIG. 7. The XRD patterns of ceramic bodies derived from Kavakbaşı clay fired at various temperatures (R = red; B = black; Mca: mica, Qtz: quartz, Kfs: K-feldspar, Pl: plagioclase, Hem: hematite, Gh: gehlenite, Di: diopside, Cal: calcite).

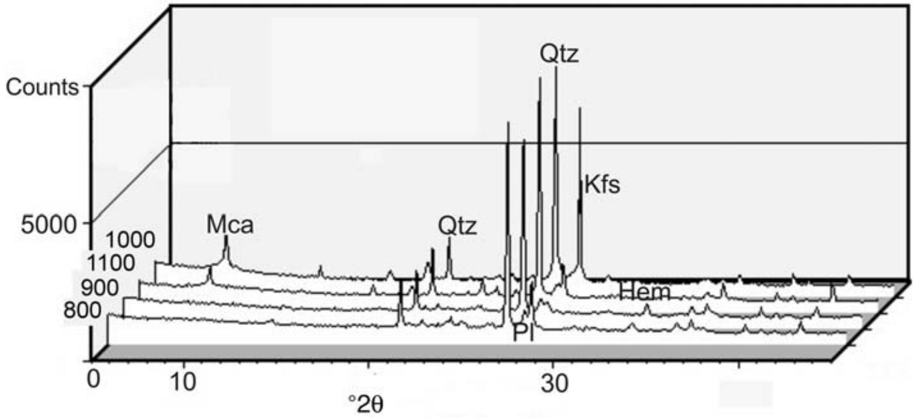

FIG. 8. XRD patterns of ceramic bodies derived from Kusluk clay fired at various temperatures (Mca: mica, Qtz: quartz, Kfs: K-feldspar, Pl: plagioclase, Hem: hematite).

glassy phase between the large mica minerals (100 μm). The EDS analyses (Fig. 10a-EDS, b-EDS) confirm the coexistence of the glassy phase and the mica minerals.

The SEM images of fresh surfaces of the Kavakbaşı body fired at 1000°C (Fig. 10c–d) show abundant circular pores which confirm the well developed glassy phase attributed to the significant Fe and alkali content in the original clay. Analysis by EDS confirmed the presence of diopside. (Fig. 10c). The glassy phase with circular pore shape (Fig. 10d) shows that melting began from the crystal surface at 1000°C.

The SEM image of the fresh surface of the Kutki body fired at 900°C (Fig. 10e–f) contains quartz and fractured plagioclase grains as was confirmed by the EDS elemental analyses (Fig. 10e–f). The SEM images of material from the Bardakçı (1000°C) Kusluk (1000°C) and Kutki (900°C) bodies show different degrees of melting of the grains and partial melting of the fine clay-minerals matrix.

Chemical composition and physical properties of ceramic test bodies of the studied clays

The Kavakbaşı, Kuşluk and Kutki carbonate-free clays and the carbonate mudstone (Bardakçı) are characterized by abundant Fe (>5.8%) and total alkalis (>3.6 %) (Table 1).

The results of the particle-size analysis of the clays are illustrated in Fig. 11 and are listed in Table 2. The analysis reveals that the Bardakçı and Kuşluk clays have a high proportion of fine particles with a relatively

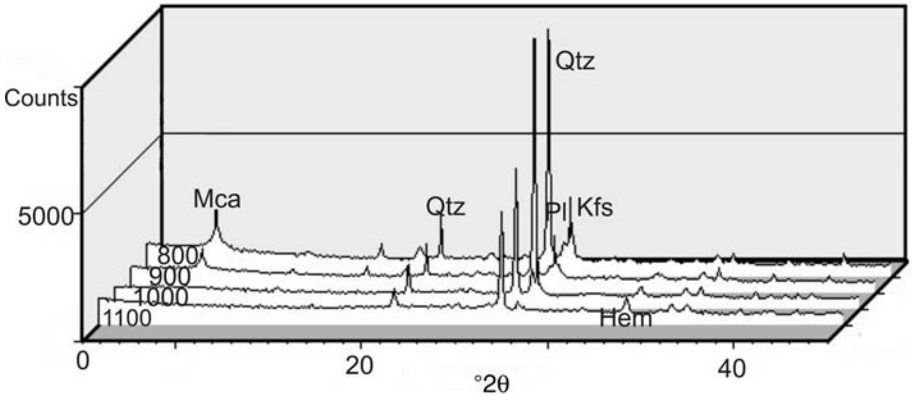

FIG. 9. XRD patterns of ceramic bodies derived from Kutki clay fired at various temperatures (Mca: mica, Qtz: quartz, Kfs: K-feldspar, Pl: plagioclase, Hem: hematite, Gh: gehlenite, Di: diopside).

https://doi.org/10.1180/claymin.2017.052.4.04 Published online by Cambridge University Press

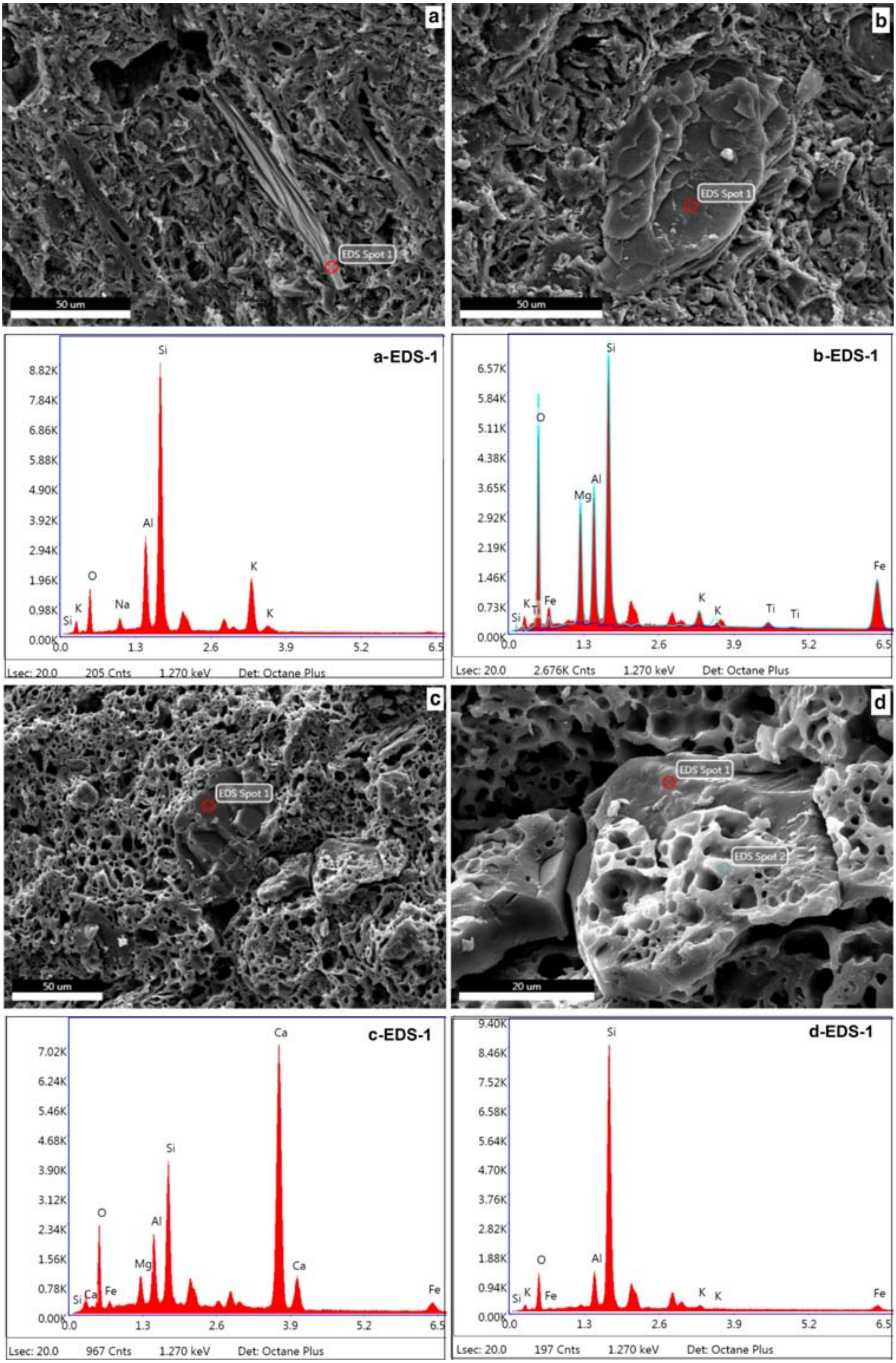

FIG. 10. Characteristic SEM microstructures and EDS elemental analyses of broken surfaces of the fired clay bodies: (a, b) Bardakçı body fired at 1000°C; (c, d) Kavakbaşı body fired at 1000°C; and (e, f) Kutki body fired at 900°C.

https://doi.org/10.1180/claymin.2017.052.4.04 Published online by Cambridge University Press

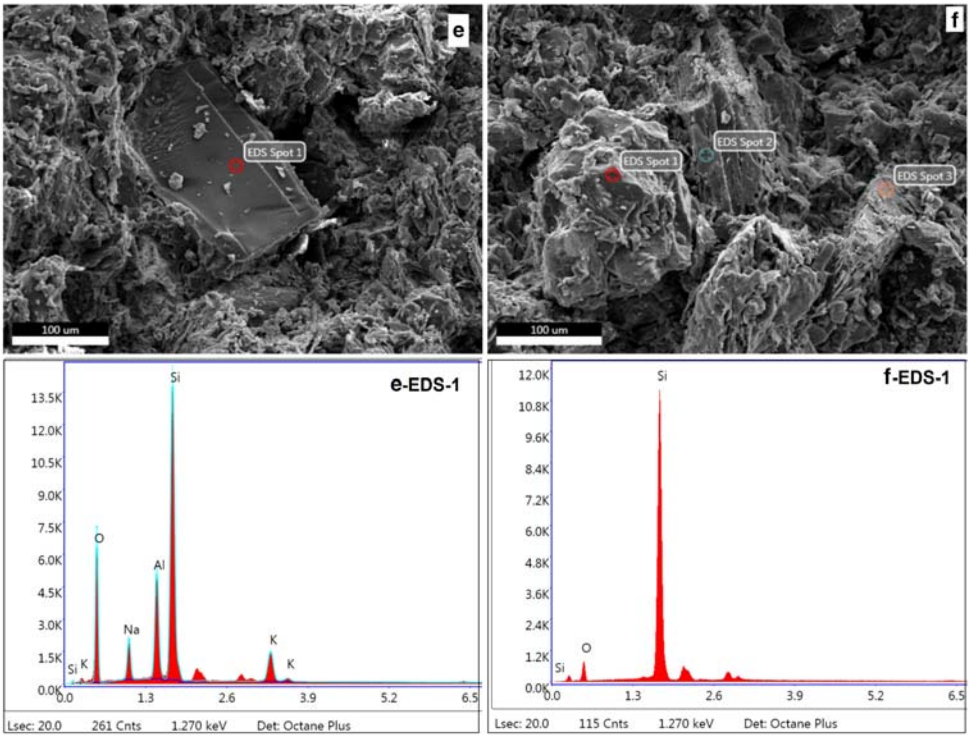

FIG. 10. Continued

narrow particle-size distribution, whereas Kavakbaşı has significant proportion of fine particles and wide and bimodal grain-size distrubution. Kutki clay contains coarser particles with a narrow range of particle-size distribution. The grain-size data were plotted in a so-called 'Winkler diagram'; the Bardakçı and Kuşluk clays are located in the 'common brick' area (Fig. 12)

During firing the original grey/green/brown colour of the clay turned to pink and reddish brown in the fired ceramic body as a consequence of the vitrification/mineralogical transformations (Table 3). The greatest lightness (*L*) and lowest redness (*a**) values were measured for the Bardakçı bodies. The absence of calcite and the large Fe content in the original clay yielded a reddish firing colour in Kutki and Kuşluk bodies which have similar *L*, *a** and *b** values (Table 3). The reddish colour observed is attributed to hematite; actually 1.0–1.5 wt.% hematite might impart a reddish colour to a fired body (Schwertmann, 1993). On the other hand, the formation of gehlenite and diopside which incorporate ferrous and/or ferric ions caused the pinkish colour in the fired Bardakçı bodies which initially contained 3.3% $CaCO_3$

TABLE 1. Major-element analysis (%) of pottery clays from Kavakbaşı, Kutki, Kuşluk and Bardakçı.

Clay	LOI	Al_2O_3	CaO	Fe_2O_3	K_2O	MgO	MnO	Na_2O	P_2O_5	SiO_2	TiO_2	ΣTotal
Bardakçı-1	7.45	19.4	3.3	5.8	2.9	3.5	0.2	1.1	0.2	55.0	0.9	99.75
Kavakbaşı-1	5.65	19.2	1.1	7.3	2.8	1.8	0.1	0.8	0.1	59.8	1.1	99.75
Kutki-1	7.20	18.6	1.5	9.2	3.0	1.9	1.2	1.1	0.2	54.7	1.1	99.35
Kuşluk-1	6.85	18.4	1.6	8.1	2.9	1.9	0.2	1.4	0.2	56.8	0.1	98.45

https://doi.org/10.1180/claymin.2017.052.4.04 Published online by Cambridge University Press

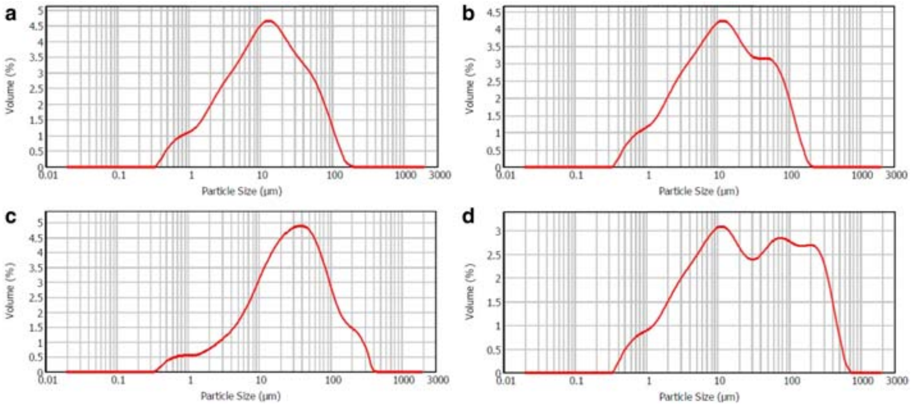

FIG. 11. Grain-size distribution curves of: (a) Bardakçı, (b) Kuşluk, (c) Kutki and (d) Kavakbaşı clay raw materials as measured by laser diffraction.

(Table 1). The maximum and minimum bending strengths were observed in the Bardakçı and Kutki test bodies, respectively.

POTTERY PRODUCTION, TRADITIONAL KILNS AND MINERALOGICAL COMPOSITION OF THE ANCIENT POT SHERDS

Sampling of clays in this study has two inherent problems: locating the clay sources and obtaining clean samples. All the pottery clay locations were located by asking local potters. For example, the Kutki clay samples were collected from the lower parts of the steep hills near Kutki village, after removing the superficial soil. The primary clayey materials derived from weathered schists are coarse-grained, characterized by illite-mica + chlorite together with feldspar and quartz which makes them unsuitable for direct use in pottery production without prior washing and settling. However, in this study the samples collected were used directly for analysis and preparation of the test bodies.

TABLE 2. The particle-size distribution of pottery clays from Kavakbaşı, Kutki, Kuşluk and Bardakçı measured using a Malvern-2000 instrument.

Clay	<2 μm	2–20 μm	>20 μm
Bardakçı	10.7	55	35
Kuşluk-1	10.9	50	38
Kavakbaşı-1	9.80	35	54
Kutki	5.20	35	60
Clay	$D_{0.1}$	$D_{0.5}$	$D_{0.9}$
Bardakçı	1.78	11.63	56.57
Kuşluk	1,75	11.98	70.35
Kavakbaşı	2.19	23.72	239.4
Kutki	3.92	22.66	121.7

$D_{0.1}$, $D_{0.5}$ and $D_{0.9}$ indicate the grain size corresponding to 10, 50 and 90 vol.% of the particles of each clay.

The low-fired, porous and unvitrified earthenware pots of Lake Van were made from a single, relatively coarse plastic, red, firing, primary clay. The earthenware pots of Lake Van represent the earliest fired pottery in the world and the two ancient pot sherds selected for this study are included in this category.

The local cultural tradition is represented by pots, their shape and their use in daily life. The maximum temperature of firing can be inferred approximately from the mineralogical composition and the microstructure of fired body, characteristics which are also affected by the firing atmosphere, however (this depends on the air circulation system in the kiln). Three types of kilns (depending on their air-circulation system) are used in the Lake Van region: the Bardakci Kiln (Fig. 13a–c), the Kavakbasi tandır (Fig. 13d–f) and the Kutki kiln (Fig. 13h). The Kavakbaşı tandır is traditional and used for baking bread in the villages of eastern and southern Anatolia. The Bardakci kiln is a circular and pyramidal kiln built with sundried mudbricks (kerpiç in Turkish) (Fig. 13a). The side walls are narrowed upwards and steps are retained on the outside. A grid exists between the lower ignition part and the upper part where the pots are placed (Fig. 13c). Also, there is a large, ~1 m, entrance to the fire

https://doi.org/10.1180/claymin.2017.052.4.04 Published online by Cambridge University Press

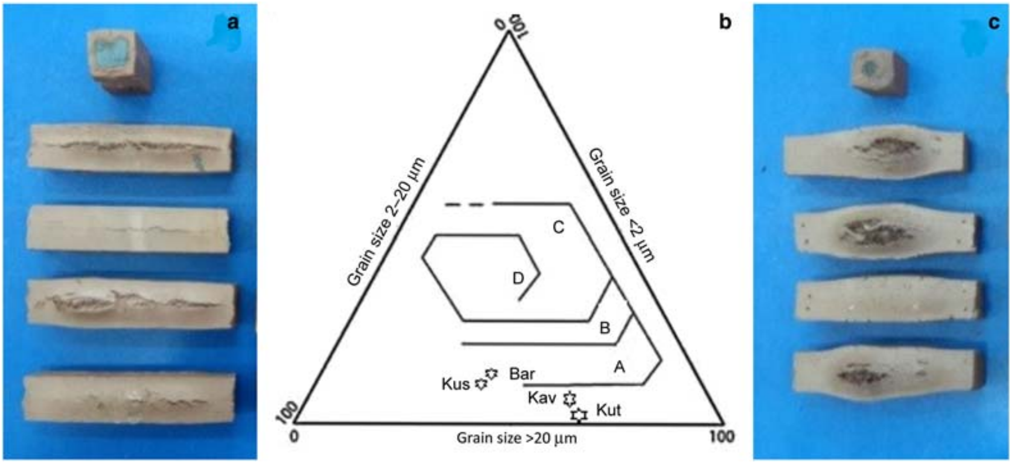

FIG. 12. (a) Development of black core in the Kavakbaşı fired test bodies at 1100°C; (b) projection of the clays studied in the Winkler diagram. [A = common bricks, B = vertically perforated bricks, C = roofing tiles and masonry bricks, D = hollow products (after Dondi *et al*., 1998]; (c) Development of black core in the Kuşluk fired test bodies at 1100°C.

chamber in the form of a deeper pit. After the dried vessels are placed in the upper part, they are covered with ceramic sherds. The red fired village pots in the vicinity of Lake Van were fired at temperatures of <900°C in these kilns. The firing time of pots is 9–10 h in the Bardakçı and Kutki kilns and 5–6 h in the Kavakbaşı tandır, but the pots were not subjected to fixed maximum temperatures as in the electrical kiln. In traditional kilns, the firing time is divided into three stages: the period when temperature is raised, the short period at which maximum temperature is sustained, and the period when no wood is added to the fire beneath the kiln – the temperature decreases and the pots cool to room temperature. The slow heating and cooling rates and the different orientations of pots in the wood-kiln cause a temperature gradient between the wall and the interior of the kiln and between the surface and the interior of pots (Fig. 13g). As a result, different physical and chemical changes take place at different times within the pot body which can set up damaging stresses. Furthermore, in the slow-rate firings at low temperatures, the pot bodies do not reach maturity; the maximum hardness and strength and the minimum porosity cannot be attained.

The investigation of wood-fired kilns at the same time as electrical kilns for firing of the same clay bodies provided a better understanding of the low-temperature procedures adopted. The same physical and chemical changes in fired clay occurred in the electrical kiln but the maximum temperature, duration and atmosphere were not controlled in wood-fired kilns. Therefore, it is not appropriate to discuss the firing technology of these simple pots by estimating temperature alone. The duration of firing at that temperature and the atmosphere in which it took place are also important. The traditional kiln technology of the Lake Van region was very simple, the atmosphere was probably very variable, neither completely oxidizing (as in the electrical kiln) nor completely reducing at any stage of firing, and may be described as incompletely oxidizing. In modern electric or gas kilns, the rate of heating can be controlled carefully and monitored up to the maximum temperature, but this is not the case for simple wood-fired kilns. In the latter the village potters control the temperature by studying the colour of the hot pot or the smoke emanating from the pots.

The XRD patterns of two ancient pot sherds from the Kutki village and the Armenian Church ruin are given in Fig. 14. The mineralogical compositions of these two sherds are similar to those of the Kutki and Kusluk ceramic bodies fired at 800–900°C. It follows that the firing temperatures of these ancient pot sherds should also be 800–900°C because of the disappearance of mica peaks at >900°C in ceramic bodies derived from the local clay. The hematite peaks were observed clearly in the ceramic test bodies. The absence of gehlenite indicates the absence of calcite in the green body or raw clay of these potteries. Finally, the broad 3.22–3.19 Å peaks indicate the presence of both K-feldspar and plagioclase.

https://doi.org/10.1180/claymin.2017.052.4.04 Published online by Cambridge University Press

TABLE 3. Physical properties of test bodies derived from the clay materials studied.

Clay		Kavakbaşı	Bardakçı	Kutki	Kuşluk	TSE*
Colour		Light brown	Light brown	Reddish brown	Reddish brown	DIN 6174
Wet sieve analysis (%)	>2.8 mm	15	10	4.2	10	TS 4790
	>0.2 mm	33	31	31	27	
Loss on ignition (%)		8.9	9.9	8.7	8.9	TS 3245
Temper grain		Rock fragments, organic matter	Calcite, organic	Rock fragments	Rock fragments, organic	TS 4790
$CaCO_3$		2	4	0	0	TS 4790
Moulding ability		Good	Very good	Good	Good	???
Plasticity water		21	23	20	24	TS 4790
Linear dry shrinkage (%)		6.8	5.3	5	5.1	TS 4790
Dry bending strength		44	48	41	45	
Firing temperature (°C)		900	800	900	900	
Firing colour		$L = 48.49$ $a^* = +14.75$ $b^* = +22.82$	$L = 53.29$ $a^* = +14.30$ $b^* = +21.81$	$L = 45.49$ $a^* = +16.75$ $b^* = +22.88$	$L = 44.86$ $a^* = +16.46$ $b^* = +22.61$	Minolta CR-300
Hardness (Mohs)		2	2.5–3	2	2	TS 4790
Total shrinkage (%)		6	7.5	6.4	6.3	TS 4790
Firing bending strength (MPa)		12.3**	13.4	11.2	12.3**	TS 4790
Compressive strength (MPa)		34	32.9	34	34	TS 4790
Bulk density (g/cm^3)		1.97	1.95	1.97	1.97	TS 771-1
Water absorption %		13.8	14.6	13.3	13.8	TS EN 771-1
Water absorption % (boiling water)		14	14.7	14	14.8	TS-EN 772-7

*Turkish Standard Institute (TSE) test used.
**Firing bending strengths measured at 800°C (the others were measured at 900°C). Higher temperatures were inappropriate for strength measurements because of the deformation of the original black core.

DISCUSSION

Properties of pottery clays in the Lake van region

The studied pottery clays of the Lake Van region include one mudstone from a lacustrine terrace deposit and three weathered Ohin schists from the metamorphic basement rocks of the Bitlis complex. The serpentine, amphibole and the large amount of smectite identified in the Bardakçı sample indicates the presence of ophiolitic rocks and clay-rich flysch rocks in source areas east of Lake Van (Fig. 1). The mineralogical composition of mudstone varied significantly even within a single level. The presence of very fine calcite in a clay fraction indicates a lacustrine environment. On the other hand, the Kutki, Kuşluk and Kavakbaşı clays on the Ohin schist (Fig. 1) show comparable mineralogical compositions. These clay samples are poor in carbonate minerals, illite-muscovite predominates and is inherited from the parent rock which was formed by weathering of mica and chlorite (Velde & Meunier, 2008). Their mineralogy differs in terms of the relative abundance of clay minerals, with smectite being more abundant in Kuşluk and Kavakbaşı than in Kutki. The disappearance of the 14 Å chlorite peak after heating at 550°C indicates strong alteration of the Ohin schist (Grim & Johns, 1954). Unlike the Bardakçı clay, in the Kusluk, Kutki and Kavakbaşı clays, *in situ* weathering is the most likely mechanism of formation of Ca-smectite (14 Å) and mixed-layer minerals. The latter might have originated from weathering caused by Na-poor, Ca-

https://doi.org/10.1180/claymin.2017.052.4.04 Published online by Cambridge University Press

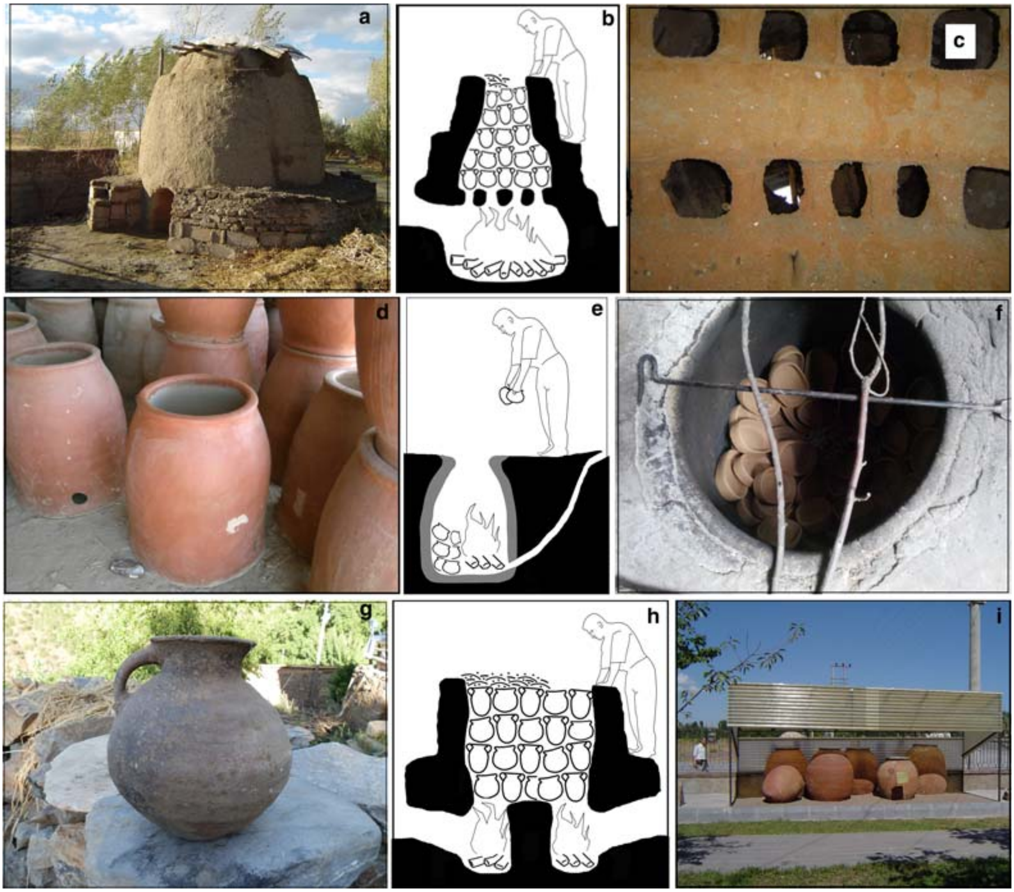

FIG. 13. (a–c) Front view, structure and inside view of an updraft kiln in Bardakçı; (d) unburied tandır at Kavakbaşı; (e) structure of a buried tandır; (f) fired güveç (special pot for baking of fish and meat) in a buried tandır; (h) Kutki pots; (g) kiln structure; and (i) pottery of the west coast of Lake Van (Ahlat).

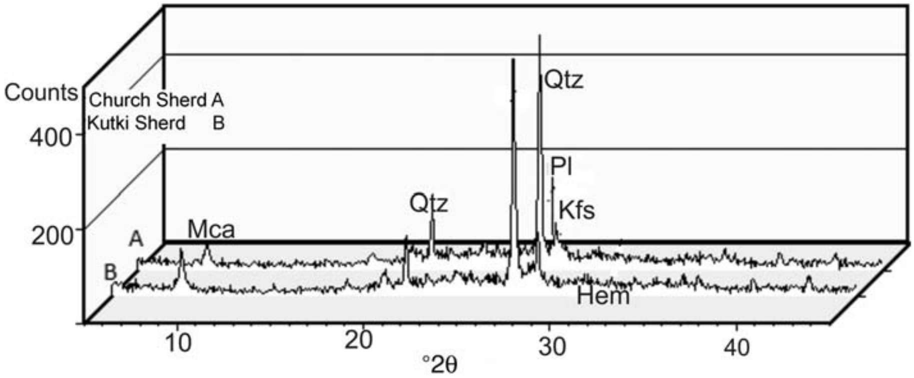

FIG. 14. XRD patterns of two ancient sherds from Kutki village and an Armenian church (Mca: mica, Qtz: quartz, Kfs: K-feldspar, Hem: hematite, Pl: plagioclase).

https://doi.org/10.1180/claymin.2017.052.4.04 Published online by Cambridge University Press

rich circulating water in terrestrial sediments (Vicente *et al.*, 1991; Wilson, 2004). The 12–15 Å peak observed in smectite indicates the effect of Na-rich pore water in the biggest sodic lake in the world, the Lake Van terrace sediment.

Relationship between the mineralogy of the clays and fired test bodies studied and the ancient sherds

The mineralogical compositions of the clays fired at 900–1000–1100°C are comparable with those fired at 800°C (Figs. 6–9). The quartz abundance decreased whereas K-feldspar and plagioclase persisted in the Bardakçı, Kavakbaşı and Kuşluk clays. Calcite and white mica are no longer present beyond 900°C in any test bodies and gehlenite, diopside and anorthite were found to increase in Kavakbaşı and Bardakçı clays. Hematite is increased for Bardakçı, Kutki, Kuşluk and Kutki at 900°C and is slightly reduced for Kavakbaşı and Kusluk because of black core formation at temperatures of >1000°C.

The effect of Ca and Mg on the mineralogical and physical properties of the ceramic bodies were studied by conventional ratios. The amount of newly formed anorthite depends on the CaO content of the green body, with maximum anorthite formation occurring in fired bodies containing 5–15% CaO at 1200°C (Schmidt & Schmidt, 1997; Dondi *et al.*, 1999; Cultrone *et al.*, 2001). Gehlenite presents its maximum at 1000°C (Dondi *et al.*, 1996). In the XRD patterns of the clays studied, the greater intensities of the plagioclase peaks at 900–1000–1100°C compared with those at 850°C are attributed primarily to the increasing contribution of anorthite (An) members (An_{0-50}) in a melting/crystallization process, where the original Na-rich plagioclase disappears progressively and a more Ca-rich plagioclase crystallizes epitaxially in Bardakçı, Kavakbaşı and Kutki (3.3% CaO in Bardakçı, 1.6% in Kutki, 1.1% in Kavakbaşı). In contrast, in Kusluk (1.5% CaO), plagioclase melts gradually and K-feldspar persists with increasing temperature. The firing behaviour of K-feldspar and plagioclase observed in the clays studied can be explained by quartz and clay solubility; a general consensus exists that quartz is more soluble in the presence of plagioclase than in the presence of K-feldspar and clay is more soluble in the presence of feldspar than it is in quartz. The melting behaviour of K-feldspar and plagioclase in kaolinite and illite-rich bodies is different: K-feldspar melted more easily in kaolinite-rich clays than did Ca-Na feldspar (Aras, 2004). The plagioclase melting in the illite-quartz Kutki clays is consistent with Aras (2004), probably because of the presence of coarse $CaCO_3$ particles in the *in situ* weathered schist of Kutki. In the case of the Bardakçı, Kuşluk and Kavakbaşı test bodies, even the small amount of finely distributed calcite caused newly formed anorthite formation in fired test bodies.

The Kavakbaşı and Kuşluk clays showed microstructural cracks and black cores at temperatures of >900°C. The cracks are due to the elevated linear shrinkage and the black core defects are due to the reaction of remaining carbon from incomplete combustion of organic matter (Fig. 12a–b). Although the Kutki and Bardakçı clay also include small amounts of carbon, in the Kutki clay, no impervious glassy skin formed on the body surface and no black core was observed because of the coarser grain-size distribution of mica, feldspar and quartz and the small amount of clay. In the case of the reworked sedimentary Bardakçı clay, the lack of a black core may be explained by the large amount of coarser rock-crystal quartz (from lacustrine and fluvial sediment), which allows carbon monoxide to escape, thus hindering black-core formation. The mullite phase was not observed in any test bodies fired because mullite forms from illite and smectite at temperatures of >1150°C (Bohor, 1963; McConville & Lee, 2005). In the illitic clay, the spinel, β-quartz and illite anhydride peaks are difficult to detect unambiguously. The Kavakbaşı clay fired at 1000°C may contain spinel.

The pottery clays from the Lake Van region are composed of illite-mica, smectite and chlorite, associated with quartz, feldspar and calcite. The large K_2O and Fe_2O_3 contents facilitated the formation of a glassy phase at low temperatures, showing low porosity and good flexural strength from 950°C onwards. With the exception of quartz and K-feldspar, which persisted up to 1100°C, with increasing firing, illite-mica, smectite, calcite and plagioclase decomposed gradually and new high-temperature phases, namely hematite, gehlenite, diopside, anorthite and spinel were formed. In addition, the colour of the ceramic bodies was controlled by the relative abundances of hematite and calcite. The mineralogical and chemical properties of clays from the Lake Van region and the physical properties of the fired test bodies derived from these clays have allowed some preliminary observations concerning their direct usage for pottery production. Thus, only Bardakçı and Kuşluk clays are located at the proper Winkler diagram region (Fig. 12b) (A) (common bricks), whereas Kutki and Kavakbaşı must be beneficiated by washing and settling prior to firing.

https://doi.org/10.1180/claymin.2017.052.4.04 Published online by Cambridge University Press

The two potsherds contain mica-sericite-illite, quartz, feldspar and hematite. Although these were probably produced during the 19–20th century, they were fired in the same updraft village kilns that are used today. The mineralogical compositions of the historical potsherds from Bardakçı, Delikli, Yılantaş, Çelebibağ, and Tilkitepe areas are free of mullite but consist of quartz, illite (probably mica-sericite-illite), feldspar, calcite and chlorite (Kılıç & Çalışkan, 2005). The presence of chlorite and calcite indicated that the firing temperatures of these historical sherds were lower than those of the updraft kiln. Akça *et al*. (2010) reported the chemical and micro-morphological observations on Urartu ceramics from 800 to 600 BC in eastern Turkey and pointed out that the raw materials in the paste of Urartu pots consisted of mica-sericite-illite and illite-smectite mixed-layer clay minerals. Those same authors indicated that the large K and Li contents in all slips relative to the bodies reveal the possible use of feldspar and/or illitic clays along with spodumene ($LiAlSi_2O_6$) and lepidolite $K(Li, Al)_{2-3}(AlSi_3O10)(O, OH,F)_2$, minerals commonly found in geological formations of the Van region (Degens *et al.*, 1984). It is possible that the Urartu clay sources in and around the Lake Van area (Çimrin *et al.*, 2004) are still utilized today for the production of the well known indigenous water-storage vessels of Van (Çilingiroğlu, 1994).

CONCLUSIONS

Examination of the mineralogical, chemical and granulometric properties of Lake Van region clays and the mineralogical and physical properties of fired test bodies derived from these clays gave rise to the following conclusions:

(1) Based on Winkler's diagram, the Bardakçı and Kuşluk clays are suitable for common brick pottery while their Kutki and Kavakbaşı counterparts might meet the Winkler's diagram standards, after adjustments to their sand-silt-clay ratios, for use in pottery production.

(2) The pottery clays studied are characterized by greater silica and lesser alumina contents than a common brick clay. On the other hand, the clays contain more Fe and alkaline elements than typical brick clays. The high proportions of Fe_2O_3 (maximum 9.2%, minimum 5.8%) are well correlated with the large mica-illite content of the four clays. Illite-mica is the dominant mineral in Kavakbaşı, Kutki and Kuşluk non-carbonate clays. The Bardakçı carbonate clays have large smectite and calcite contents.

(3) The XRD and SEM-EDS data of the clays studied showed that the bulk compositions of the Kutki, Kusluk and Kavakbaşı clays included feldspar and mica which have large percentages of Fe and alkalis compared to the Bardakçı sample. This reduced the melting point and improved glass formation at temperatures of >900°C. At all firing temperatures, fresh fractured surfaces were not compact, having pores between mineral grains, because of the large amount of flux minerals in batch mineralogical compositions. The firing test performed on individual clay bodies which have high alkali and Fe contents showed that the optimum vitrification temperature for pottery production is 900°C. In the calcite-containing Bardakçı body, diopside, akermanite and gehlinite formed as part of a solid-solution series of minerals.

(4) The mineralogical, chemical and granulometric analyses and the physical properties of fired test bodies derived from the clays of Lake Van region demonstrated the possibility of establishing the presence of two different ceramic pastes, namely metamorphic and ophiolitic-volcanic. The former is characterized by a calcite-poor, mica-sericite-rich matrix together with quartz, K-feldspar and plagioclase (two types of feldspar) and the latter is characterized by rock crystal quartz and large amounts of smectite and calcite.

(5) The mineralogical compositions of the two ancient sherds indicate firing temperatures of 800–900°C and a metamorphic paste because of the presence of resistant mica minerals and the absence of gehlenite minerals.

REFERENCES

Akça E., Arocena J., Kılıç S., Dingil M. & Kapur S. (2010) Preliminary chemical and micromorphological observations on Urartu (800–600 B.C.) Ceramics, Eastern Turkey. *Geoarchaeology*, **25**, 233–244.

Altınlı İ.E. (1966) Doğu ve Güneydoğu Anadolu'nun Jeolojisi. *M.T.A. Dergisi*, 527–588.

Aras A. (2004) The change of phase composition in ceramic bodies in kaolinite- and illite-rich clay based ceramic bodies. *Applied Clay Science*, **24**, 257–269.

Bohor B.F. (1964) High temperature phase development in illitic clays. *Clay and Clay Minerals,* **12**, 233–244.

https://doi.org/10.1180/claymin.2017.052.4.04 Published online by Cambridge University Press

Burney C.A. (1958) Eastern Anatolia in the Chalcolithic and Early Bronze Age. *Anatolian Studies*, **VIII**, 157–209.

Çilingiroğlu A. (1994) The Second Millennia BC Colored Pottery Produced in the Lake Van Basin. *Ege Üniversitesi Arkeoloji Dergisi*, **2**, 1–3 (in Turkish).

Çimrin K.M., Akça E., Şenol M., Büyük G. & Kapur S. (2004) Potassium potential of the soil of Gevaş region, East Anatolia. *Turkish Journal of Agriculture and Forestry*, **28**, 259–266.

Cultrone G., Rodriguez-Navarro C., Sebastian E., Cazalla O. & De la Torre M.J. (2001) Carbonate and silicate phase reactions during ceramic firing. *European Journal of Mineralogy*, **13**, 621–634.

Degens E.T. & Kurtman F. (1978) *The Geology of Van*. MTA Publications No. **169**, Ankara, pp. 50–55.

Degens E.T., Wong H.K., Kempe S. & Kurtman F. (1984) A geological study of Lake Van, Eastern Turkey. *International Journal of Earth Sciences*, **73**, 701–734.

Dondi M., Ercolani G., Fabbri B. & Marsigli M. (1996) Chemistry of pyroxene and melilite formed during the firing of ceramic clay bodies. Pp. 210–211 in: *Advances in Clay Minerals, Proceedings of the Spanish–Italian Meeting on Clay Minerals*, Granada, Spain.

Dondi M., Fabbri B. & Guarini E. (1998) Grain-size distribution of Italian raw materials for structural clay products: a reappraisal of the winkler diagram. *Clay Minerals*, **33**, 435–442.

Dondi M., Guarini G. & Raimondo M. (1999) Trends in the formation of crystalline and amorphous phases during the firing of clay bricks. *Tile & Brick Internationl*, **15**, 19.

Göncüoğlu M.C. & Turhan N. (1984) Geology of the Bitlis metamorphic belt. Pp. 237–244 in: *Proceedings of the International Symposium on the Geology of the Taurus Belt* (O. Tekeli & M.C. Göncüoğlu, editors). Mineral Research and Exploration Institute, Ankara, Turkey.

Grim R.E. & Johns W.D. (1954) Clay minerals investigation of sediments in the northern Gulf of Mexico. Clays and Clay Minerals, Publication **327**, National Academy of Science, National Research Council, pp. 81–103.

Kapur S., Sakarya N. & Fitzpatrick E.A. (1992) Mineralogy and micromorphology of Chalcolithic and Early Bronze Age Ikiztepe ceramics. *Geoarchaeology*, **7**, 327–337.

Kılıç S. & Çalıskan N. (2005) Determination of the clay mineral assemblages of the prehistoric pottery of the Van Basin by XRD analysis. Pp. 110–120 in: *Proceedings of the 12th National Clay Symposium*, September 5–9, 2005, Van, Turkey.

Korfmann M. (1982) *Tilkitepe. Die ersten Ansätze prähistorischer Forschung in der östlichen Türkei*, *Istanbuler Mitteilungen Beiheft* 26. Verlag Ernst Wasmuth, Tübingen, Germany.

Kuzucuoğlu C., Christol A., Mouralis D. & Doğu A.F. (2010) Formation of the Upper Pleistocene terraces of Lake Van (Turkey). *Journal of Quaternary Science*, **25**, 1124–1137.

McConville C.J. & Lee W.E. (2005) Microstructural development on firing illite and smectite compared with that in kaolinite. *Journal of the American Ceramic Society*, **88**, 2267–2276.

Oberhänsli R., Candan O., Bousquet R., Rimmele G., Okay A. & Goff J.B. (2010) Alpine HP Evolution of the Eastern Bitlis Complex, SE Turkey. Pp. 461–483 in: *Sedimentary Basin Tectonics from the Black Sea and Caucasus to the Arabian Platform* (M. Sosson, N. Kaymakci, R.A. Stephenson, F. Bergerat & V. Starostensko, editors). Special Publications, 340, Geological Society of London.

Okay A., Arman M.B. & Göncüoğlu M.C. (1985) Petrology and phase relations of the kyanite-eclogites from Eastern Turkey. *Contributions to Mineralogy and Petrology*, **91**, 196–204.

Oyan V. & Tolluoğlu Ü. (2005) *Na-feldspar-rich Leucogranitic Rocks in the Bitlis Massif (Yolcular Metamorphic): A Potential Source for Feldspar*. Yerbilimleri/Hacettepe Üniversitesi Yerbilimleri Uygulama ve Araştırma Merkezi Dergisi, Ankara, cilt.26, ss.1–11.

Sakarya N., Kapur S. & FitzPatrick E.A. (1990) Preliminary study of the microstructure and mineralogy of 12th and 13th century ceramics, Samsat, southeastern Turkey. *Geoarchaeology*, **5**, 275–281.

Schmidt-Reinholz Ch. & Schmidt H. (1997) The effect of lime and dolomite in brick bodies and finished products Part 1–2. *Tile & Brick International*, **13,** 14–17, 110–114.

Schwertmann U. (1993) Relationships between iron oxides, soil color and soil formation. Pp. 51–69 in: *Soil Color 31* (J.M. Bigham & E.J. Ciokosz, editors). Soil Science Society of America, Madison, Wisconsin, USA.

Standard: DIN 6174 (2007) Colorimetric evaluation of color coordinates and color differences according to the approximately uniform CIE-Lab color space.

Thorez J. (1976) Qualitative Determination of mixed Layers. Pp. 42–46 in: *Practical Identification of Clay Minerals* (G. Lelote, editor). Editions, Liege, Belgium.

TSE-BS-EN 771-1 (2007) Specification for masonry units. Clay masonry units.

TSE-BS-EN 772-7 (2015) Methods of test for masonry units - Part 7: Determination of water Absorption of clay masonry damp proof course units by boiling in water.

TSE-Standard TSE 4790 (1998) Test method for common bricks and roofing tile clays.

Velde B. & Meunier A. (2008) *The Origin of Clay Minerals in Soils and Weathered Rocks*. Springer, Berlin, Heidelberg, 406 pp.